International Journal of Advances in Engineering and Management (IJAEM)
Volume 4, Issue 2 Feb 2022, pp: 1574-1583 www.ijaem.net ISSN: 2395-5252

Application of Response Surface Methodology for Optimization of Phenol Degradation in Photo-Fenton process by Nano Zero Valent Iron Composite

I.A. Ndanusa[1], B.O. Aderemi [2], A. Hamza[2], D.B. Hassan [3]

[1]*Department of Chemical Engineering, Kaduna Polytechnic, Kaduna, Nigeria*
[2]*Department of Chemical Engineering, Ahmadu Bello University, Zaria, Nigeria*
[3]*Centre for Energy Research and Training, Ahmadu Bello University, Zaria, Nigeria*

Submitted: 15-02-2022 Revised: 25-02-2022 Accepted: 28-02-2022

ABSTRACT: In this study, the effectiveness of nano zero-valent iron (nZVI) composite on Photo-Fenton degradation of phenol was evaluated. The experimental results indicate that nanocomposite under the light influence enhance phenol degradation efficiency up to 98.8%. Response Surface Methodology (RSM) using Central Composite Design (CCD) was performed byDesign expert V12 software to determine the optimum operating conditions for Phenol degradation efficiency. The process variables optimized wereH_2O_2 concentration, catalyst dose, degradation time and phenol concentration. From the Analysis of Variance (ANOVA)show that phenol degradation is most influenced by degradation time, followed by catalyst and H_2O_2 concentration. The predicted degradation efficiency was found in good agreement with the experimental value, with coefficient of determination (R_2) = 0.9756. The best condition that maximizes phenol degradation are 8.816 mmol/L H_2O_2 concentration, 0.139 g/L catalyst, 115.433 min degradation time and 19.535 mg/L phenol concentration at maximum desirability of 1 to give about 100% phenol degradation efficiency.

KEYWORDS: Photo-Fenton Process, Phenol Degradation, Nano Zero Valent Iron (nZVI), Response Surface Methodology (RSM), Optimization, and Central Composite Design (CCD).

I. INTRODUCTION

Large amount and a wide variety of organic and inorganic compounds are produced in the chemical industry, many of them persistent, toxic, and non-biodegradable [1]. Phenols occupy a prominent place among the pollutants of ground waters and large part of it is caused by industry [2]. Due to the wide utilization in different industries, e.g. chemical, petrochemical, paint, textile, pesticide plants, phenols have become the most abundant pollutants in industrial wastewater [3]. They serve as intermediates in the industrial synthesis of products and their presence contributes notably to the pollution of the effluents due to their high toxicity to aquatic life, and may cause carcinogenic and mutagenic effects to humans [4]. Removing these compounds from industrial wastewaters, or especially from natural groundwater or soil if released is challenging [1,5]. The Fenton's reagent is widely used to degrade chemicals in water due to simplicity and low-cost [1,4]. In the classic Fenton reaction, a combination of H_2O_2 and Fe^{2+} ions are used at low pH to produce hydroxyl radicals [6], which oxidize organic compounds; however, low pH has to be maintained to prevent Fe^{3+} precipitation and the concentration of H_2O_2 and Fe^{2+} are relatively high, which can inhibit organic material degradation due to radical scavenging [6]. To overcome these drawbacks, much attention has been focused in recent years on the development of iron containing heterogeneous catalysts for the various oxidation processes [7]. The advantage of using nZVI in the Fenton reaction is that these limitations can be overcome, and nZVI is able to reduce oxygen on its surface leading to hydroxyl radicals, therefore, peroxide free Fenton-type reactions can be conducted for organic material degradation [8]. Although it has been well established that Fenton processes based on nZVI show high efficiency in degrading organic pollutants

International Journal of Advances in Engineering and Management (IJAEM)
Volume 4, Issue 2 Feb 2022, pp: 1574-1583 www.ijaem.net ISSN: 2395-5252

under controlled reaction conditions [9]. There are several variants of this heterogeneous Fenton reaction, where the main role of nZVI is the generation of reactive radical species such as $OH^{\cdot}, O_2^{\cdot-}, SO_3^{\cdot-}$ and $SO_5^{\cdot-}$. Leaching and precipitation of iron, however, cannot be avoided in these reactions what limits the reusability of the catalyst different types of nano zero valent iron- supported on bentonites intercalated with organic and inorganic cations have been synthesized [13,14,15].

Conventionally, wastewater treatments, like many other industrial processes are optimized by using "one at a time" variation of treatment variables [16]. Moreover, this method assumes that various treatment parameters do not interact and that the response variable is only function of the single varied parameter[17]. However, the response obtained from a waste treatment method for example, results from the interactive influences of the different variables [18]. When a combination of several independent variables and their interactions affect desired responses, response surface methodology (RSM) is an effective tool for optimizing the process [19]. RSM uses an experimental design such as the central composite design (CCD) to fit a model by least squares technique [20]. Adequacy of the proposed model is then revealed using the diagnostic checking tests provided by analysis of variance (ANOVA). The response surface plots can be employed to study the surfaces and locate the optimum. In several industrial processes, RSM is almost routinely used to evaluate the results and efficiency of the operations [21]. The primary objective of optimization in this study was to find the best input conditions that maximizes phenol degradation. The Design Expertv12 application package was used to determine the optimum parameter that maximizes phenol degradation using the desirability function with the setup constraint for degradation time, catalyst, H_2O_2 concentration and phenol concentration in range between the lower and upper limit.

II. METHODOLOGY

2.1 Materials and Analytical Methods

Sodium borohydride (NaBH4), iron(III) chloride hexahydrate ($FeCl_3{\cdot}6H_2O$); Aluminum(III) chloride hexahydrate ($AlCl_3.6H_2O$); Sulfuric acid (H_2SO_3), sodium hydroxide (NaOH), absolute ethanol (C_2H_5OH) (99%); and Phenol (99%) were obtained from Merck India. Nanoscale zero-valent iron supported on pillared bentonite (nZVI-PILB) was synthesized by ferric iron reduction method using sodium borohydride as a reducing agent under ethanol medium at atmospheric conditions. [10]. Furthermore, nZVI particles are more prone to oxidation to form Fe2O3 or Fe3O4, leading to agglomeration into large particles, which makes the processes such as separation, recovery and recycling more difficult [11]. To eliminate these problems, supporting materials are used to immobilize nZVI as an alternative strategy [12]. Over the last few years,

2.2 Experimental Design and Optimization

Preliminary experiments were performed with an initial phenol concentration of 20 mg/L, an initial H_2O_2 concentration of 10 mmol/L, a catalyst dose of 0.3 g/L, and pH 5.5 for various reaction times. In each experiment, the suspension was stirred for 30 min in the dark to achieve the equilibrium of adsorption/desorption between the catalyst and phenol. About 10.0 mL of the suspension was sampled and immediately filtered using vacuum filtration to separate catalysts from solution, the concentration of phenol in the supernatant was measured using gas analyzer, then a 40 W halogen lamp was switched on, and the Photo-Fenton catalytic degradation was started [22]. At given time intervals, aliquots of the solution and about 10.0 mL were sampled and immediately filtered by vacuum filtration to remove catalyst. Residual H_2O_2 in these samples was immediately quenched with 0.1 mol/L of Na_2SO_3, in other to avoid the occurrence of Fenton reaction through the possible presence of leached iron. Samplings were done at different intervals as specified by the Design expert software for analysis and phenol degradation efficiency of was calculated using the following equation:

$$\text{Degradation efficiency} = \left[\frac{CO-Ct}{CO}\right] 100$$

A four factor Split-Plot Central Composite Design (CCD) with 5 levels (plus and minus alpha (axial points), plus and minus 1 (factorial points) and the center point) was utilized. The factors selected as independent variables are H_2O_2 concentration, catalyst dose, degradation time and phenol concentration, and are selected based on report from previous studies. The experimental design was developed using Design Expert 12 application package [19]. The uncoded levels of the independent variables are shown in Table 1.

To achieve the optimization study and to analyze the effect of input factors (H_2O_2 concentration, X_1, catalyst, X_2, degradation time, X_3 and phenol concentration, X_4) and interactions on the response degradation efficiency, a second (quadratic) polynomial model was utilized as shown in equation 1.

$$Y = \beta_o + \beta_1X_1 + \beta_2X_2 + \beta_3X_3 + \beta_4X_4 + \beta_{12}X_1X_2 + \beta_{13}X_1X_3 + \beta_{14}X_1X_4 + \beta_{23}X_2X_3 +$$

International Journal of Advances in Engineering and Management (IJAEM)
Volume 4, Issue 2 Feb 2022, pp: 1574-1583 www.ijaem.net ISSN: 2395-5252

$\beta_{24}X_2X_4 + \beta_{34}X_3X_4 + \beta_{11}{X_1}^2 + \beta_{22}{X_2}^2 + \beta_{33}{X_3}^2 + \beta_{44}{X_4}^2$ (1)

where

$\beta_{i,j}$= coefficient of model terms, X_1 = H_2O_2 concentration, X_2 = catalyst, X_3 = degradation time, X_4 = phenol concentration and Y = degradation efficiency, which is the response variable and it is defined as shown in equation 2.

$$Y(\%) = \frac{C_0 - C}{C_0} \times 100 \quad (2)$$

where C_0= initial concentration of phenol, C = concentration of phenol after each experimental run

III. RSULTS AND DISCUSSION

3.1 Split-Plot Experimental Design

The result of the experimental design for the input factors (H_2O_2 concentration, catalyst, degradation time, and phenol concentration) are presented in Table 2. The t-distribution, coefficients and p-values for the experimental results were obtained and the sum of squares as well as the F-distribution were also determined. The 95% confidence level was used for the statistical calculations.

Table 1: Uncoded level of the independent variables

Factor	Units	Change	Low	High	-alpha	+alpha
H_2O_2 Concentration	mmol/L	Easy	5	25	-5	35
Catalyst	g/L	Easy	0.1	1	-0.35	1.45
Time	min	Easy	20	120	-30	170
Phenol Concentration	mg/L	Hard	10	20	5	25

Table 2: Experimental design matrix and response factor of split-plot CCD analysis of oil yield

		Factors				Response		
Group	Run	A: H_2O_2 Conc. (mmol/L)	B: Catalyst (g/L)	C: Time (min)	D: Phenol Conc. (mg/L)	Phenol Degradation (%) Actual	Predicted	Residual
1	1	15	-0.35	70	15	70	67.70	2.30
1	2	15	0.55	170	15	98	91.93	6.07
1	3	15	0.55	-30	15	3.85	4.32	-0.47
1	4	35	0.55	70	15	80	73.57	6.43
1	5	-5	0.55	70	15	60	60.83	-0.83
1	6	15	1.45	70	15	87	83.70	3.30
2	7	15	0.55	70	5	79	82.63	-3.63
2	8	15	0.55	70	5	80	82.63	-2.63
3	9	5	0.1	20	20	32	35.33	-3.33
3	10	5	0.1	120	20	90	93.89	-3.89
3	11	25	0.1	120	20	82	99.00	-17.00
3	12	5	1	120	20	52	63.14	-11.14
3	13	25	1	120	20	85	85.15	-0.15
3	14	5	1	20	20	36	42.93	-6.93
3	15	25	0.1	20	20	32.5	36.69	-4.19
3	16	25	1	20	20	50	61.19	-11.19
4	17	15	0.55	70	15	98.5	98.66	-0.16
4	18	15	0.55	70	15	98.6	98.66	-0.06
4	19	15	0.55	70	15	98.7	98.66	0.04
5	20	15	0.55	70	25	78	72.63	5.37
5	21	15	0.55	70	25	76	72.63	3.37
6	22	15	0.55	70	15	98.8	98.66	0.14
6	23	15	0.55	70	15	98.7	98.66	0.04
6	24	15	0.55	70	15	98.7	98.66	0.04
7	25	5	0.1	20	10	33.8	31.98	1.82
7	26	5	1	20	10	70	61.83	8.17
7	27	25	0.1	20	10	25	22.70	2.30

International Journal of Advances in Engineering and Management (IJAEM)
Volume 4, Issue 2 Feb 2022, pp: 1574-1583 www.ijaem.net ISSN: 2395-5252

7	28	25	0.1	120	10	98.7	90.10	8.60
7	29	25	1	120	10	93	98.50	-5.50
7	30	5	0.1	120	10	98	95.64	2.36
7	31	25	1	20	10	75	69.45	5.55
7	32	5	1	120	10	93	87.14	5.86
8	33	15	0.55	70	15	98.5	98.66	-0.16
8	34	15	0.55	70	15	98.8	98.66	0.14
8	35	15	0.55	70	15	98.6	98.66	-0.06

Regression Model and Analysis

Table 3 presents the regression model coefficient of the response variable (phenol degradation efficiency, Y) in terms of coded factors. The regression model in term of coded factors shown in Table 3, is expressed in equation 3.

$$Y = 98.65556 + 3.18333A + 4B + 21.90417C - 2.5010d + 4.225AB + 0.9375AC + 2.6625Ad - 9.5875BC - 5.5625Bd - 1.275Cd - 7.86359A^2 - 5.73859B^2 - 12.63234C^2 - 5.25583d^2 \quad (3)$$

The regression model in terms of actual factors as represented in equation 4 is suitable for predicting the response phenol degradation efficiency for any given levels of each factor in its actual terms with the levels specified in their original units for individual factor

$$Y = -49.739278 + 1.241679X_1 + 93.082236X_2 + 1.430220X_3 + 6.624525X_4 + 0.938889X_1X_2 + 0.001875X_1X_3 + 0.053250X_1X_4 - 0.426111X_2X_3 - 2.472222X_2X_4 - 0.005100X_3X_4 - 0.078991{X_1}^2 - 28.514154{X_2}^2 - 0.005067{X_3}^2 - 0.218760{X_4}^2 \quad (4)$$

The fitness and validity of the regression model with experimental response was evaluated using the regression coefficient, R^2 and Adjusted-R^2. The obtained regression coefficients, R^2 and Adjusted-R^2 value of the fitted regression model are 0.9756 and 0.9538 respectively. This shows that the 97.56% of the experimental data are well captured and describable by the regression model. The high R2 and Adjusted-R2 value of the model confirms that the quadratic model of the central composite split-plot RSM adequately describe the experimental data and suitable for predicting the response phenol degradation efficiency. The coefficient of variation (CV) obtained in this study is 9.046%, further confirms the suitability and better precision of the model to describe experimental data.

The plot of the predicted against actual experimental response denoted by the colored point all lays very close to the diagonal line representing the predicted response in Figure 3a, indicating the validity and goodness of the fitted regression model for predicting phenol degradation efficiency [23,24]. The normal probability plot shows organized and cluster points that are very close to the diagonal line in Figure 3b, suggesting the homogeneity of the error discrepancies and the independent style of the residuals which signifies that the errors are normally distributed and independent of each other.

Table 3: Model coefficient in terms of coded factor

Source	Coefficient Estimate	Standard Error	VIF
Intercept	98.66	3.16	
Whole-plot Terms:			
d- Phenol Conc.	-2.50	1.80	1.0000
d^2	-5.26	1.29	1.09
Subplot Terms:			
A-H_2O_2 Conc.	3.18	1.02	1.0000
B-Catalyst	4.00	1.02	1.0000
C-Time	21.90	1.02	1.0000
AB	4.22	1.25	1.0000
AC	0.9375	1.25	1.0000
Ad	2.66	1.25	1.0000
BC	-9.59	1.25	1.0000
Bd	-5.56	1.25	1.0000
Cd	-1.27	1.25	1.0000

International Journal of Advances in Engineering and Management (IJAEM)
Volume 4, Issue 2 Feb 2022, pp: 1574-1583 www.ijaem.net ISSN: 2395-5252

A^2	-7.86	1.39	1.80
B^2	-5.74	1.39	1.80
C^2	-12.63	1.39	1.80
R^2	0.9756		
Adjusted-R^2	0.9538		
Coefficient of Variation (CV)	9.05 %		

Analysis of Variance (ANOVA)

The regression model was validated statistically using ANOVA to confirm the adequacy of the model and to identify importance of the model and its parameters. The significance of the factors and the model were evaluated using p-value and F-value which is a means of assessing the interaction strength and effect of each parameter as well as the model. If the p-value is < 0.05, then the factor and/or model is statistically significant at the 95% confidence level while p-value is > 0.05 is not significant [25] The split-plot ANOVA for the fitted regression model is summarized in Table 4.

Table 4 also shows that the Sub-Plot F-value is 54.78 with p-value < 0.0001, a further confirmation that the model is highly significant (p-value < 0.05) with only a 0.01% chance that a 54.78 F-values could occur due to noise in the experimental data (25,26 and 27]. The Sub-plot terms of the model are A (H_2O_2 concentration), B (catalyst), C (time), AB, AC, Ad, BC, Bd, Cd, A^2, B^2 and C^2. It can be seen that A, B, C, AB, Ad, BC, Bd, A^2, B^2 and C^2 are significant model terms with p-values < 0.05. However, the model term AC and Cd do not have significant effect on the response variable as their p-values are greater than 0.100. Since theinsignificant model terms are not being many, model reduction may not necessarily improve the model

.

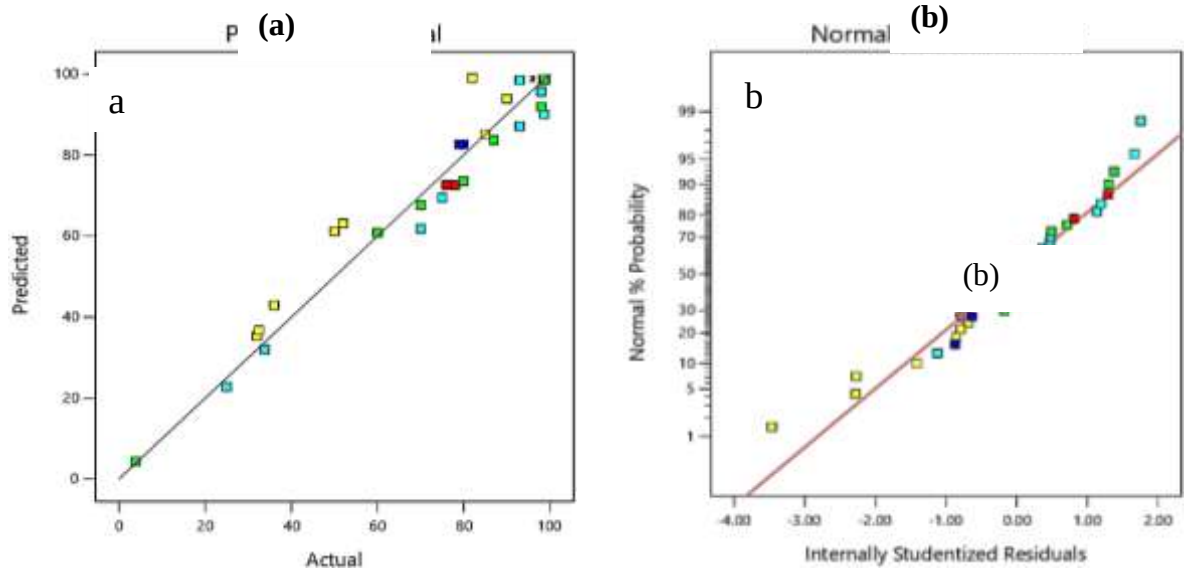

Figure 3: Diagnostics plot of model: (a)Predicted vsActual plot of response, and (b) Normal probability of residuals.

Table 4: ANOVA for split-plot CCD quadratic model

Source	Term df	Error df	F-value	p-value	Remark
Whole-plot	**2**	**5.60**	**9.30**	**0.0166**	**Significant**
d- Phenol Conc.	1	5.43	1.93	0.2191	Not significant
d^2	1	5.79	16.68	0.0070	Significant
Subplot	**12**	**14.18**	**54.78**	**< 0.0001**	**Significant**

International Journal of Advances in Engineering and Management (IJAEM)
Volume 4, Issue 2 Feb 2022, pp: 1574-1583 www.ijaem.net ISSN: 2395-5252

A-H_2O_2 Conc.	1	16.38	9.68	0.0066	Significant
B-Catalyst	1	16.38	15.28	0.0012	Significant
C-Time	1	16.38	458.35	< 0.0001	Significant
AB	1	16.38	11.37	0.0038	Significant
AC	1	16.38	0.5597	0.4650	Not significant
Ad	1	16.38	4.51	0.0492	Significant
BC	1	16.38	58.54	< 0.0001	Significant
Bd	1	16.38	19.71	0.0004	Significant
Cd	1	16.38	1.04	0.3237	Not significant
A^2	1	7.61	32.13	0.0006	Significant
B^2	1	7.61	17.11	0.0036	Significant
C^2	1	7.61	82.91	< 0.0001	Significant

Response Surface Analysis

Figure 2a showed that phenol degradation increases with increase in catalyst and H_2O_2 concentration to reach a maximum degradation efficiency, which is attributed to the availability of HO^- for degradation reaction [17]. Further increase in the catalyst and H_2O_2 concentration to 1 g/L and 25 mmol/L respectively resulted in slight decrease in phenol degradation efficiency, which is due to the attainment of saturation point and scavenging effect of the catalysts on the reactive HO^- radical. Also, the contour line shown in Figure 2a is an indication that the plot is quadratic and suggests that the interaction between catalyst and H_2O_2 concentration have significant effect on phenol degradation which is in conformity with results presented in Table 4.

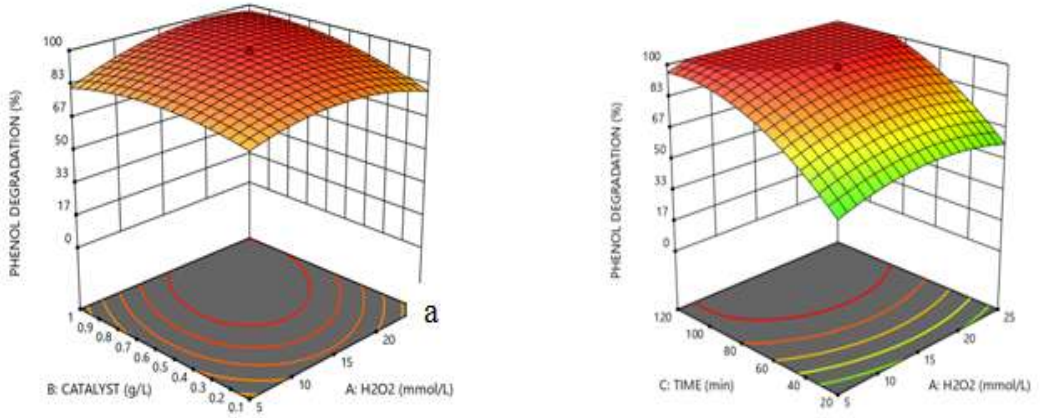

Figure 2: 3D Surface plot for; (a) effect of catalyst and H_2O_2 concentration, and (b) effect of time and H_2O_2 concentration on phenol degradation.

Figure 2b showed that phenol degradation increases rapidly with increase in time and slightly with increase in H_2O_2 concentration to reach a maximum degradation efficiency, which is attributed to availability of sufficient degradation time and HO- for degradation reaction. However, further increase in time beyond 70 min do not show significant effect on phenol degradation efficiency while increase in H_2O_2 concentration to 25 mmol/L show a slight decrease form the maximum degradation efficiency attained.

Figure 3a showed that phenol degradation efficiency increases with rise in both phenols concentration and H_2O_2 concentration to attain maximum degradation efficiency, further rise in both phenol concentration and H_2O_2 concentration result in a gradual reduction in phenol degradation efficiency. The rise in response variable to a maximum with increase in both phenol

International Journal of Advances in Engineering and Management (IJAEM)
Volume 4, Issue 2 Feb 2022, pp: 1574-1583 www.ijaem.net ISSN: 2395-5252

concentration and H_2O_2 concentration is attributed to the production of more hydroxyl radicals during degradation which enhance the degradation efficiency [27, 28]

Similarly, Figure 3b showed rapid rise in phenol degradation with increases in both degradation time and catalyst. The rise in phenol degradation to almost 100% is due to availability of more degradation site on the catalysts, effective surface area of the catalyst and sufficient degradation time [29, 30]. This shows that interaction between degradation catalyst and time have the most influence on phenol degradation efficiency which corroborate the ANOVA analysis of effect (Table 4).

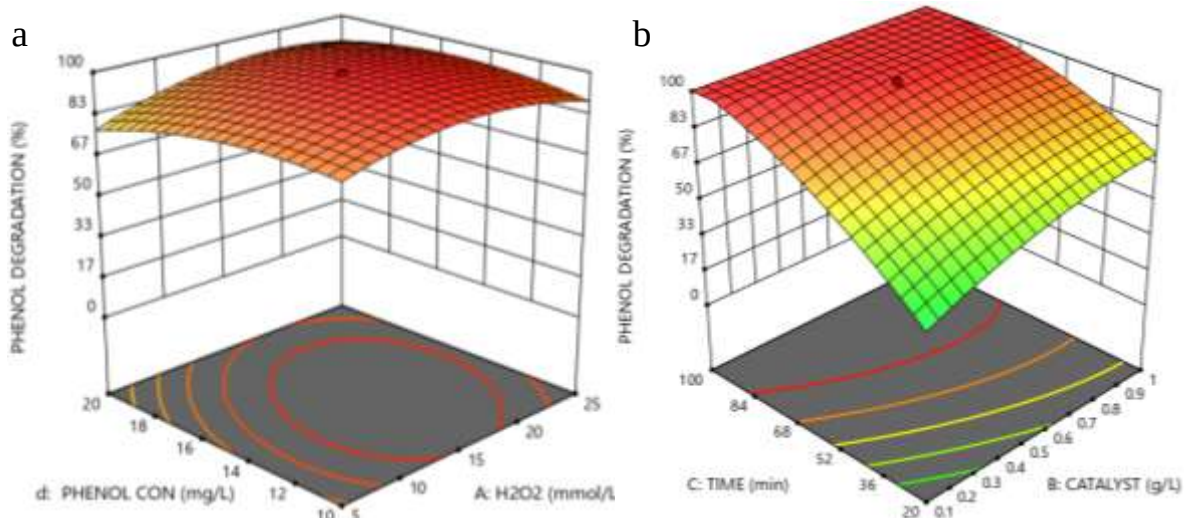

Figure 3: 3D Surface plot for; (a) effect of phenol concentration and H_2O_2 concentration, and (b) effect oftime and catalyst on phenol degradation

Figure 4a presents the surface plot of the influence of both phenol concentration and catalyst on phenol degradation. Increases in both phenol concentration and catalyst, increases phenol degradation with catalyst having the most influence. However, further increase in phenol concentration 15 mg/L resulted in a decrease in degradation rate, which is due to increased number of phenol molecules and OH- radicals compared to active catalyst site available when phenol concentration increases [27]. In Figure 4b increase in degradation time have the most influences on phenol degradation efficiency compared to phenol concentration. This is attributed to the availability of sufficient time for more phenol degradation [28].

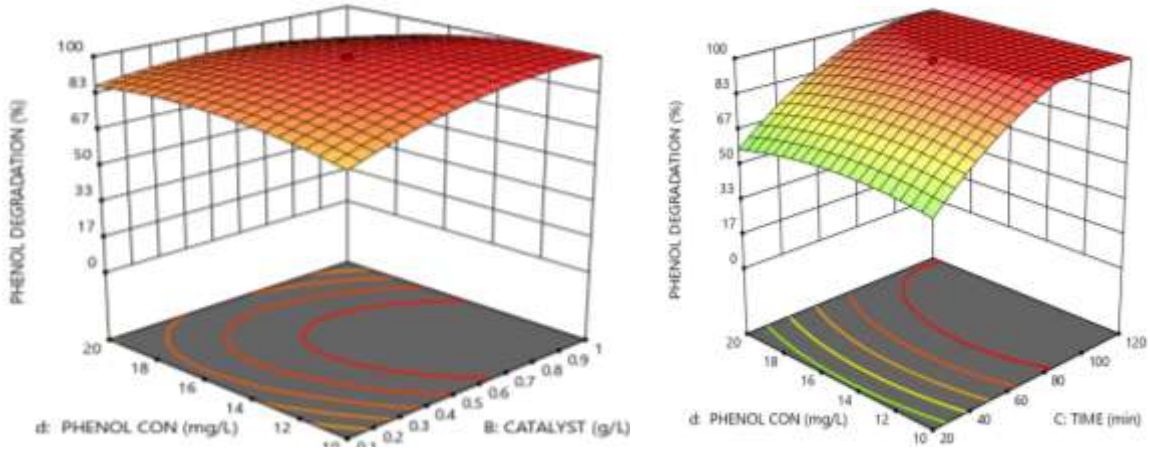

(a) (b)

Figure 4: (a) effect or pnenol concentration & catalyst, (b) effect of phenol concentratıon & time

International Journal of Advances in Engineering and Management (IJAEM)
Volume 4, Issue 2 Feb 2022, pp: 1574-1583 www.ijaem.net ISSN: 2395-5252

Optimum Process Parameter

Table 5 shows the result of the optimization showing the factor setting, predicted responses and desirability. The best condition that maximizes phenol degradation are 8.816 mmol/L H_2O_2 concentration, 0.139 g/L catalyst, 115.433 min degradation time and 19.535 mg/L phenol concentration at maximum desirability of 1 to give about 100% phenol degradation efficiency.

Table 5: Split-plot CCD optimization result

Number	H_2O_2 Conc.	Catalyst	Time	Phenol Conc.	Phenol Degradation	Desirability	
1	19.133	0.835	114.244	17.534	100.000	1.000	
2	24.468	0.983	116.565	10.073	100.000	1.000	
3	**8.816**	**0.139**	**115.433**	**19.535**	**100.000**	**1.000**	**Selected**
4	24.789	0.169	119.686	19.852	100.000	1.000	
5	20.167	0.476	76.745	15.273	100.000	1.000	
6	11.495	0.930	105.028	13.564	100.000	1.000	
7	10.678	0.114	110.583	10.449	100.000	1.000	
8	20.724	0.816	100.449	18.134	100.000	1.000	
9	22.848	0.273	114.337	10.930	100.000	1.000	
10	23.729	0.110	106.631	17.635	100.000	1.000	
11	8.223	0.148	118.695	10.161	100.000	1.000	
12	24.655	0.927	79.000	11.173	100.000	1.000	
13	15.625	0.353	83.720	11.723	100.000	1.000	
14	8.892	0.854	98.586	11.170	100.000	1.000	
15	17.425	0.778	108.661	18.227	100.000	1.000	

IV. CONCLUSION

Optimization of catalytic degradation of phenol was investigated using Split-plot CCD response surface method. The study examines H_2O_2 concentration, catalyst, time and phenol concentration as input factor to maximize phenol degradation efficiency. The Split-plot CCD response surface method shows that phenol degradation is most influenced by degradation time, followed by catalyst and H2O2 concentration while phenol concentration shows the least influence on degradation efficiency. The best condition that maximizes phenol degradation are 8.816 mmol/L H_2O_2 concentration, 0.139 g/L catalyst, 115.433 min degradation time and 19.535 mg/L phenol concentration at maximum desirability of 1 to attain almost a 100% phenol degradation efficiency.

REFERENCES

[1]. Tibor P. and Melinda K., 2020, "Synthesis and Application of Zero-Valent Iron Nanoparticles in Water Treatment, Environmental Remediation, Catalysis, and Their Biological Effects. Nanomaterials review

[2]. Hrvoje C., Natalija., Ana L. B., Iva S., 2006, "Photo-assisted Fenton type processes for the degradation of phenol: A kinetic study" Journal of Hazardous Materials B136 632–644

[3]. Alnaizy R., and Akgerman A., 2000, "Advanced oxidation of phenolic compounds", Advance Environmental Resource 4 (3) p. 233–244.

[4]. Arjunan B. and Karuppan M. 2011, "Degradation of Phenol in Aqueous Solution by Fenton, Sono-Fenton and Sono-Photo-Fenton." Journal of Clean Soil, Air, Water 39 (2), 142

[5]. Arjunan B. A., and Karuppan M. 2012, "Removal of phenol by heterogeneous photo electro Fenton-like process using nano-zero valent iron". Journal of Separation and Purification Technology 98: 130–135

[6]. Karim, S.; Bae, S.; Greenwood, D.; Hanna, K.; Singhal, N. 2017, "Degradation of ethinylestradiol by nano zero valent iron under dierent pH and dissolved oxygen levels". Water Res. 125, 32–41.

[7]. Rui C. M., André F. R., and Rosa M. Q. 2010, "Fenton's oxidation process for phenolic wastewater remediation and biodegradability enhancement". Journal of Hazardous Materials 180: 716–721

[8]. Khalil H., Tiangoua K., and Christian R. 2010, "Fenton-like oxidation and mineralization of phenol using synthetic Fe(II)–Fe(III) green rusts", journal of

Environmental Science Pollution Resource 17:124–134

[9]. Arjunan B. A., and Karuppan M. 2012, "Removal of phenol by heterogeneous photo electro Fenton-like process using nano-zero valent iron" Journal of Separation and Purification Technolog 98: 130–135

[10]. Rezaei, F. Vione, D. 2018, "effect of pH on zero valent iron performance in heterogeneous Fenton and Fenton-like processes": A review. Molecules 2018, 23, 3127

[11]. Rui C. M., André F. R., and Rosa M. Q. 2010, "Fenton's oxidation process for phenolic wastewater remediation and biodegradability enhancement" Journal of Hazardous Materials 180: 716–721

[12]. Yuvakkumara R, Elangoa V, Rajendrana V, and N. Kannan N. 2011, "Preparation and Characterization of Zero Valent Iron nanoparticles"; Journal of Nanomaterials and Biostructures Vol. 6, No 4, p. 1771-1776

[13]. Adusei-Gyamfi, J., &Acha, V. 2016, "Carriers for nanozerovalent iron (nZVI): Synthesis, application and efficiency. RSC Advances, 6(93), 91025–91044.

[14]. Jianfa L, Yimin L. Qingling M. 2010, "Removal of nitrate by zero-valent iron and pillared bentonite" Journal of Hazardous Materials 174, 188–193

[15]. Yun Zhanga,b, Yimin L, Jianfa L, Liujiang H, Xuming Z. 2011, "Enhanced removal of nitrate by a novel composite: Nanoscale zero valent iron supported on pillared clay", "Chemical Engineering Journal 171 (2011) 526– 531

[16]. Muthukumar M., Sargunmani D., SelvakumarN., and J. Venkata Rao J. 2004, "Optimisation of ozone treatment for colour and COD removal of acid dye effluent using central composite design experiment," Dyes Pigments, vol. 63, pp. 127-134.

[17]. Ayodele, O. B., Lim, J. K. and Hameed, B. H. (2012). Degradation of phenol in Photo-Fenton process by phosphoric acid modified kaolin supported ferric-oxalate catalyst: Optimization and kinetic modeling. Chemical Engineering Journal, 197, p. 181 – 19.

[18]. Yasaman G., Nishesh K., Jiyeol B. and Kwang S. 2019, "Heterogeneous Catalytic Performance and Stability of Iron-Loaded ZSM-5, Zeolite-A, and Silica for Phenol Degradation: A Microscopic and Spectroscopic Approach" Journal of Applied catalysis

[19]. Suvanka D., Ananya G., Sankar C., and Rajnarayan S. 2015, "Application of Response Surface Methodology for Optimization of Reactive Azo Dye Degradation Process by Fenton's Oxidation". International Journal of Environmental Science and Development, Vol. 6, No. 11,

[20]. Mason R.L., Gunst R.F., Hess J.2003, "Statistical Design and Analysis of Experiments with Applications to Engineering and Science", John Wiley and Sons Inc. (An International Thomason Publishing, Europe, London, 1V7AA), Hoboken, NJ.

[21]. Ahmadi M., Vahabzadeh F., Bonakdarpour B., Mofarrah E., Mehranian M., 2005, "Application of the central composite design and response surface methodology to the advanced treatment of olive oil processing wastewater using Fenton's peroxidation". Journal of Hazardous Materials B12, 187–195

[22]. Lian Y, Jiandong C, Zhen L, Weicheng X, Limin C. 2016, "Degradation of phenol using Fe3O4-GO nanocomposite as a heterogeneous Photo-Fenton catalyst" journal of Separation and Purification Technology

[23]. Shehu, M. S. Lamido, S. I. and Alhassan, A. U. 2019, "Optimization of Double Transesterification for Biolubricant Synthesis from Jatropha Oil". International Advanced Research Journal in Science, Engineering and Technology. Vol. 6, Issue 5, p. 24 – 29. DOI10.17148/IARJSET.2019.6505.

[24]. Bazezew, A. M., Emire, S. A., Sisay, M. T. and Teshome P. G. 2022, "Optimization of mucilage extraction from Ximeniaamericana seed using response surface methodology". Heliyon, Vol. 8, e08781: 1 – 8. https://doi.org/10.1016/j.heliyon.2022.e08781

[25]. Montgomery, D. C. 2013, "Design and Analysis of Experiments". 8th edition, Hoboken, New Jersey: Wiley. ISBN 978-1119320937

[26]. Maqsood, Z. and Ibrahim, M. 2015, "The Significance of P-Value in Medical Research". Journal of Allied Health Sciences, Pakistan, 1(1):74-85.

[27]. Tetteh, E. K., Rathilal, S. and Naidoo, D. B. 2020, "Photocatalytic Degradation of Oily

Waste and Phenol from A Local South Africa Oil Refinery Wastewater Using Response Methodology" Nature Research Scientific Reports,10:8850, https://doi.org/10.1038/s41598-020-65480-5

[28]. Rana, A. G. and Minceva, M. 2021, "Analysis of Photocatalytic Degradation of Phenol with Exfoliated Graphitic Carbon Nitride and Light-Emitting Diodes Using Response Surface Methodology"Catalysts, 11(898), p. 8 – 14. https://doi.org/10.3390/catal11080898

[29]. Echabbi, F., Hamlich, M., Harkati, S., Jouali, A., Tahiri, S. and Lazar, S. 2019, "Photocatalytic Degradation of Methylene Blue by The Use of Titanium Doped Calcined Mussel Shells CMS/TiO2". Journal of Environment and Chemical Engineering, 7 (5), p. 103293

[30]. Yigezu, M. B., Tafere, A. B. and Mohammed, S. B. 2021, "Optimization and Characterization of Calcinated Chicken Egg Shell Doped Titanium Dioxide Photo Catalyst Based Nanoparticles for Wastewater Treatment". Water Conservation & Management, 5(2), p. 79 – 83.